*polysaccharides*

MDPI

*Article*

# Low Molecular Weight Fucoidan Ameliorates ADHD-like Symptoms in Spontaneously Hypertensive Rats Through Neurochemical and Gut Microbiota Modulation

**Yueyang Leng [1,2,3], Jing Wang [1,2,3], Ning Wu [1,2,3], Yang Yue [1,2,3], Lihua Geng [1,2,3] and Quanbin Zhang [1,2,3,*]**

[1] Laboratory of Experimental Marine Biology, Institute of Oceanology, Chinese Academy of Sciences, Qingdao 266071, China; lengyueyang20@mails.ucas.ac.cn (Y.L.); jingwang@qdio.ac.cn (J.W.); wuning@qdio.ac.cn (N.W.); yueyang@qdio.ac.cn (Y.Y.); lhgeng@qdio.ac.cn (L.G.)
[2] Laboratory for Marine Biology and Biotechnology, Qingdao Marine Science and Technology Center, Qingdao 266071, China
[3] University of Chinese Academy of Sciences, Beijing 100049, China
* Correspondence: qbzhang@qdio.ac.cn

## Abstract

Attention deficit hyperactivity disorder (ADHD), a prevalent neurodevelopmental disorder characterized by inattention, impulsivity, and hyperactivity, is associated with monoaminergic dysfunction, neuronal damage, and gut microbiota disorders. Low molecular weight fucoidan (LMWF) is a sulfated polysaccharide extracted from *Saccharina japonica* (Phaeophyta), processes antioxidant, anti-inflammatory, and neuroprotective properties, suggesting its potential relevance for ADHD-related pathophysiology. This study investigated the therapeutic effects of LMWF on ADHD-like symptoms in spontaneously hypertensive rats (SHR). Behavioral tests revealed that LMWF reduced hyperactivity and anxiety-related behavior in the open field test, and improved spatial memory in the Morris water maze test. LMWF treatment significantly increased dopamine (DA), norepinephrine (NE), and 5-hydroxyindoleacetic acid (5-HIAA) levels in the prefrontal cortex (PFC). The transcript levels of tyrosine hydroxylase (*Th*) and synaptosome-associated protein-25 (*Snap25*) were upregulated, while dopamine transport (*Dat*) was downregulated in the PFC. TH protein expression was elevated in the striatum (STR), and neuronal integrity was preserved in the STR and cerebellum. LMWF also reshaped gut microbiota composition and enhanced microbial diversity, contributing to improved gut-brain axis homeostasis. These findings suggest that LMWF may serve as a promising dietary intervention for ADHD through neurochemical restoration and microbiota modulation.

**Keywords:** attention deficit hyperactivity disorder; low molecular weight fucoidan; dopamine system; spontaneously hypertensive rats; brain-gut axis



Academic Editor: Karin Stana Kleinschek

Received: 31 December 2025
Revised: 31 May 2026
Accepted: 2 June 2026
Published: 4 June 2026



## 1. Introduction

Attention deficit hyperactivity disorder (ADHD) is a prevalent neurodevelopmental disorder characterized by inattention, impulsivity, and hyperactivity [1]. In China, ADHD affects approximately 6.4% of children and adolescents, often persisting into adulthood and imposing a significant socioeconomic burden [2].

Although abnormalities in several brain regions and disturbances of the catecholaminergic pathway have been demonstrated, the pathophysiology of ADHD is not completely

understood. As a multifactorial disorder, current research highlights several key pathological mechanisms, including neurotransmitter abnormalities, oxidative stress, neuroinflammation, dysregulation of the gut-microbiota-brain axis, and mitochondrial dysfunction [3,4]. The pathogenesis of ADHD is primarily involving the dysregulation of monoaminergic neurotransmitter systems, particularly dopamine (DA) and norepinephrine (NE), within the prefrontal cortex (PFC) and striatum (STR) [5,6]. The clinical efficacy of dopaminergic medications further supports the key role of impaired dopamine transmission. In addition, imbalances in other monoamines, such as norepinephrine and serotonin (5-HT), are associated with impulsivity and attention deficits. Besides neurotransmitter abnormalities, increasing evidences suggests that oxidative stress and neuroinflammation may also contribute to ADHD pathogenesis [7]. Meanwhile, the role of the gut-microbiota-brain axis in ADHD has been increasingly explored, although its precise contribution remains under investigation [8].

Current pharmacological interventions such as methylphenidate and atomoxetine are widely used in the clinical management of ADHD. However, their long-term use is frequently limited by adverse effects, including insomnia, appetite suppression, and potential cardiovascular risks [9,10]. These limitations highlight the need for alternative or complementary therapeutic strategies. Consequently, increasing attention has been directed toward natural bioactive compounds capable of targeting multiple pathological processes in ADHD, including neurotransmitter dysregulation, oxidative stress, and neuroinflammation [11].

Low molecular weight fucoidan (LMWF), a sulfated polysaccharide derived from *Saccharina japonica* (Phaeophyta), has gained prominence for its diverse biological activities, including potent antioxidant, anti-inflammatory, and neuroprotective properties [12–14]. Previous studies have demonstrated that LMWF can modulate dopaminergic signaling, including restoring dopamine levels and upregulating tyrosine hydroxylase (TH) expression in catecholaminergic dysfunction models [15,16]. Furthermore, LMWF has been reported to influence gut microbiota composition and reduce neuroinflammatory responses, suggesting that it may act through multiple biological pathways. However, its potential effects on ADHD-like phenotypes and the underlying mechanisms remain to be fully elucidated.

The spontaneously hypertensive rat (SHR) is well-established genetic model of ADHD, exhibiting core phenotypes, including hyperactivity, impulsivity and attention deficits [17,18]. The Wistar–Kyoto (WKY) rat serves as the normotensive control due to its shared genetic background, enabling controlled comparisons [19,20]. SHR rats display ADHD-like behavioral and neurochemical abnormalities prior to hypertension onset, supporting their validity as a neurodevelopmental model [18,21,22], and they respond to clinically effective ADHD medications [18]. Although hypertension develops at 7–15 weeks [23], ADHD-like behaviors emerge at 3–4 weeks. Therefore, juvenile SHR (4–6 weeks old) are widely used as a pre-hypertensive model [24,25], avoiding confounding effects of elevated blood pressure. Despite concerns regarding their complex genetic background, SHR remain the most widely accepted and extensively used model in ADHD research.

In this study, the therapeutic effects of LMWF on ADHD-like symptoms were evaluated using the SHR model, with WKY rats serving as normotensive controls. Behavioral, neurochemical, molecular, and microbiota-modulating effects of LMWF were systematically investigated to provide a scientific basis for its potential as a natural dietary intervention for ADHD management.

## 2. Materials and Methods

### *2.1. Reagents and Antibodies*

Atomoxetine hydrochloride was purchased fromEli Lilly and Company, Indianapolis, IN, USA; standards of neurotransmitters, including dopamine (DA), norepinephrine (NE), 5-hydroxytryptamine (5-HT), high vacuum apparatus (HVA), 5-hydroxyindole acetic acid (5-HIAA), $\gamma$-aminobutyric acid (GABA), acetylcholine (ACh), glutamic acid (Glu), glycine (Gly), tyrosine (Tyr), were purchased from Sigma-Aldrich (Darmstadt, Germany).

Low molecular weight fucoidan (LMWF) derived from *Saccharina japonica* was prepared in laboratory according to a previously reported method [14]. Briefly, crude fucoidan extracted from *S. japonica* was depolymerized using an ascorbate–hydrogen peroxide solution (30 mmol/L, 1:1) for 2 h. The resulting solution was then subjected to DEAE Sepharose Fast Flow column chromatography for fractionation. Fractions eluted with 1 M NaCl were collected, concentrated, and designated as LMWF. The monosaccharide composition of LMWF primarily consisted of fucose and galactose with a molar ratio of 3:1. The fucose content was 33.14%, and the sulfate content was 29.30%. The weight–average molecular weight of LMWF was 7.2 kDa.

### *2.2. Experimental Animal Groups and Drug Administration*

Four-week-old male WKY ($n$ = 10) and SHR ($n$ = 40) were obtained from Beijing Vital River Laboratory Animal Technology Co., Ltd. (Beijing, China, Certificate No. SCXK(Jing)2021-0006). After a 5–day acclimatization period, all animals were weighed and evaluated using the open field test (OFT). SHRs were randomly assigned to four groups ($n$ = 10 in per group). The model group (Mod) received physiological saline by gavage. The positive group (Pos) received atomoxetine hydrochloride (5 mg/Kg/day) by gavage for 3 weeks [8,26]. The LMWFL and LMWFH groups received LMWF at doses of 100 mg/Kg/day and 300 mg/Kg/day, respectively. WKY rats served as the normal control group (Con, $n$ = 10) and were administered physiological saline by oral gavage. The dosages and route of administration of LMWF were selected based on previous published studies [27,28]. A schematic timeline of the experimental procedure is illustrated in Figure 1A. All behavioral tests were conducted between 6:30 PM and 10:30 PM local time to ensure consistency with their natural circadian rhythm.

Animals were housed in polycarbonate cages (3–4 rats per cage) under standard laboratory conditions (temperature: 22 $\pm$ 3 °C, relative humidity: 60 $\pm$ 5%, 12-h light-dark cycle). All rats had ad libitum access to sterilized standard pellet chow and purified water. All animal procedures were carried out in accordance with the *Guidelines for the Care and Use of Laboratory Animals* issued by the Ministry of Health of the People's Republic of China (Documentation No. 55, 2001), and adhered to internationally accepted principles for the ethical use of laboratory animals. The study was conducted in compliance with the ARRIVE guidelines. The experimental protocol was reviewed and approved by the Animal Ethics Committee of Qingdao University (Approval No. 20211126SHR10020220115006) on 21 October 2021.

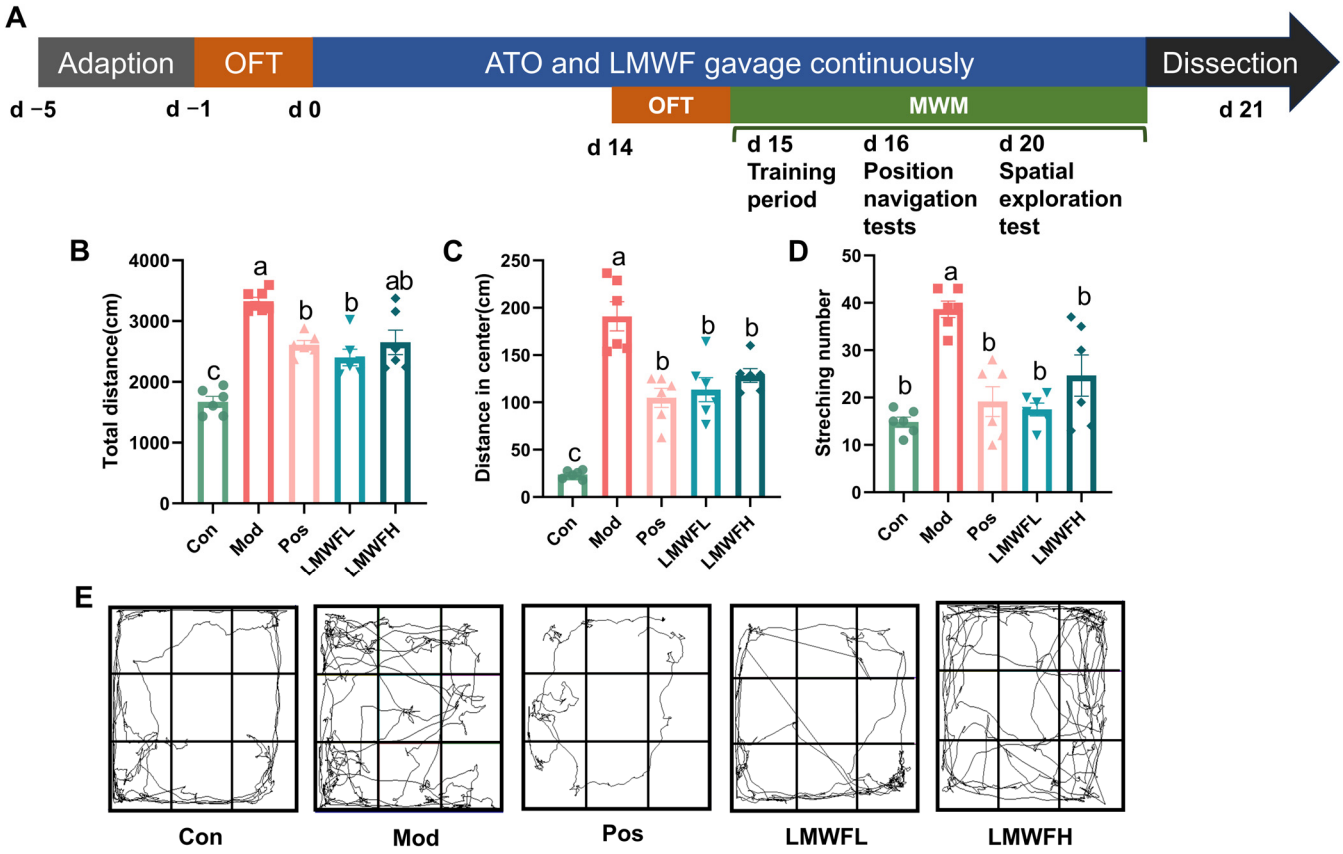


**Figure 1.** Regulation of LMWF on anxiety and hyperactivity behavior of animals evaluated by the Open Field test. (**A**) Experimental timeline showing acclimation, behavioral testing, drug administration, and sample collection. (**B**) Total distance traveled (cm). (**C**) Distance traveled in the center area (cm). (**D**) Stretching number. (**E**) Representative movement trajectories of each group. Data are presented as mean ± SEM ($n \geq 6$). Groups sharing the same letter are not significantly different, while groups labeled different letters differ significantly ($p < 0.05$). OFT, the open field test; MWM, the Morris water maze; d, day; WKY, Wistar-Kyoto rats; SHR, spontaneously hypertensive rats; ATO, atomoxetine; LMWF, low molecular weight fucoidan; Con, the control group of WKY animals; Mod, the model group of SHR animals without treatment; Pos, the positive group of SHR animals with ATO treatment; LMWFL, the group of SHR animals with 100 mg/kg/day LMWF treatment; LMWFH, the group of SHR animals with 300 mg/kg/day LMWF treatment.

### *2.3. Behavioral Tests*

#### 2.3.1. Open Field Test (OFT)

The OFT was conducted on day 0 and after two weeks of drug administration to assess spontaneous locomotor activity, exploratory behavior, and anxiety-like responses, as previously described [29]. The apparatus consisted of a 50 × 50 × 50 cm square arena [30] equipped with an overhead video camera connected to a behavioral tracking system (Smart V3.0.0.6, Panlab, Barcelona, Spain).

Each rat was placed in the center of the arena, which was virtually divided into a 3 × 3 grid. Behavior was recorder for 5 min. Parameters measured included total distance traveled, central zone distance, number of stretch-attend postures. Tests were performed in a blinded manner to avoid bias [31]. The arena was cleaned with 70% ethanol between trials to eliminate olfactory cues. The behavioral room was maintained under dim lighting (~10 lux), with ambient noise levels kept below 65 dB [32].

2.3.2. Morris Water Maze (MWM) Test

Following the OFT, MWM was employed to assess spatial learning and memory function, as previously described [33]. The system comprised a circular pool (diameter 180 cm, height 50 cm) filed with opaque black water (25 ± 1.0 °C) [34]. A transparent escape platform (diameter 20 cm) was submerged 2 cm below the surface in quadrant III. For the position navigation phase, rats were released from random quadrants and allowed 120 s locate the hidden platform. Escape latency and success rates were recorded over consecutive training sessions [35]. In the spatial exploration test, the platform was removed, and rats were allowed to swim freely for 60 s from quadrant I. Metrics included latency to the first platform crossing, time and distance spent in the target quadrant, and number of platform crossings [36]. All trials were recorded and analyzed using automated tracking software to ensure objectivity and precision.

### *2.4. Tissue Collection and Brain Slice Preparation*

After behavioral testing, animals were anesthetized and sacrificed via abdominal aortic bloodletting ($n$ = 6 per group). The prefrontal cortex (PFC) and striatum (STR) were collected and stored at −80 °C for biochemical analysis. Colon feces were collected in sterile EP tubes and frozen at −80 °C for microbiota analysis [37].

For histology, rats ($n$ = 4 per group) were perfused transcardially with 0.9% saline followed by 4% paraformaldehyde (PFA). Brains were post-fixed in 4% PFA at 4 °C for 2–3 days, washed with PBS, and cryoprotected in 30% sucrose. Paraffin-embedded coronal brain sections (5 μm) were prepared for further analysis [38].

### *2.5. LC/MS Analysis*

The LC-MS/MS analysis was performed for the simultaneous quantification of monoamine neurotransmitters in the PFC and STR of rats. Brain tissues were homogenized in methanol: acetonitrile (1:1, $v/v$), followed by centrifugation at 12,000 rpm for 10 min at 4 °C. The supernatants were spiked with 1/10 volume of 200 nM 2-pyridylacetic acid hydrochloride as an internal standard (IS) [39].

Neurotransmitters were quantified using a liquid chromatography-tandem mass spectrometry (LC-MS/MS) system, consisting of an HPLC (Shimadzu, Kyoto, Japan) and a triple quadrupole mass spectrometer (Triple Quad 4500, SCIEX, Framingham, MA, USA), operated with Analyst 1.6.2 software (SCIEX). Chromatographic separation was performed on an ACQUITY UPLC® BEH Shield RP18 column (2.1 × 100 mm, 1.7 μm) at 25 °C. The mobile phases were 0.1% aqueous formic acid as solution A, and acetonitrile as solvent B. The gradient program was as follows: 0–2 min, 2% B; 2–3 min, 2% B to 90% B;3–5 min, 90% B; 5–6 min, 90% B to 2% B; 6–10 min, 2% B [40]. The injection volume was 20 μL. Detection was conducted in positive ion mode using electrospray ionization (ESI). Multiple reaction monitoring transitions for quantification and confirmation were optimized and are listed in Table 1. Key MS parameters were as follows: curtain gas, 30.0; collision gas, 8; ion spray voltage, 5500.0; temperature, 370.0; ion source gas 1, 30.0; ion source gas 2, 0.0.

**Table 1.** List of multiple reactions monitoring parameters. Reprinted with permission from Ref. [8], Publisher Yueyang Leng, 2025.

| Analyte | Q1 Mass ($m/z$) | Q3 Mass ($m/z$) | DP(V) | CE(V) |
|---|---|---|---|---|
| DA | 154.1 | 137.2 | 50 | 15 |
| NE | 170.1 | 152.2 | 90 | 10 |
| 5-HIAA | 192.1 | 146.1 | 60 | 20 |

**Table 1.** *Cont.*

| Analyte | Q1 Mass (*m*/*z*) | Q3 Mass (*m*/*z*) | DP(V) | CE(V) |
|---|---|---|---|---|
| HVA | 183.1 | 137.1 | 90 | 25 |
| ACh | 146.1 | 87.1 | 80 | 20 |
| GABA | 104 | 87.1 | 30 | 15 |
| Tyr | 182 | 123 | 50 | 40 |
| Glu | 148.1 | 84.1 | 80 | 15 |
| Gly | 76 | 30 | 40 | 20 |
| IS | 137.9 | 120.1 | 25 | 25 |

### 2.6. Quantitative Real-Time PCR

To evaluate the regulatory effects of LMWF on the transcription of key neural pathway genes, quantitative real-time PCR (qRT-PCR) was performed on PFC issue. Total RNA was extracted using the FastPure® Cell/Tissue Total RNA Isolation Kit V2 (Vazyme Biotech, Nanjing, China), following the manufacturer's protocol. RNA (300 ng) was reverse-transcribed using the HiScript® III RT SuperMix for qPCR (+gDNA wiper) (Vazyme Biotech, Nanjing, China) [41]. qRT-PCR was carried out on a QuantStudio 6 Flex Real-Time PCR System (Applied Biosystems, Foster City, CA, USA) using ChamQ Universal SYBR qPCR Master Mix (Vazyme Biotech, Nanjing, China). Relative mRNA expression levels of *Th*, *Dat*, and *Snap25* were designed based on validated mRNA sequences from the NCBI database. They were normalized to *Gapdh* and calculated using the Livak method ($2^{-\Delta\Delta Ct}$) [42]. Primer sequences were synthesized by Sangon Biotech (Shanghai, China), and are listed in Table 2.

**Table 2.** DNA sequences of primers used in qRT-PCR.

| | Accession No. | Forward Primer | Reverse Primer |
|---|---|---|---|
| *Gapdh* | NM_017008.4 | TTCACCACCATGGAGAAGGC | CTCGTGGTTCACACCCATCA |
| *Th* | NM_012740.3 | TCCCAGGACATTGGACTTGC | AAGCCTTCAGCTCCCCATTC |
| *Dat* | NM_012694.2 | GTCACCAACGGTGGCATCTA | AATTGCTGGACGCCGTAGAA |
| *Snap25* | NM_030991.2 | AGTCACACAAGGCTACCAGC | GTGGCTTTGGAGGCAAACAG |

### 2.7. Hematoxylin and Eosin (H&E) Staining

To evaluate the histopathological changes in brain tissues, paraffin-embedded sections (5 µm thick) of the striatum (STR) and cerebellum (CE) were subjected to H&E staining. Briefly, the sections were deparaffinized in xylene twice (10 min each) and rehydrated through a series of graded ethanol solutions (100%, 95%, 80%, and 70%) for 5 min at each step [43]. After washing with distilled water, the sections were stained with hematoxylin solution for 5 min, followed by rinsing in running tap water. The sections were then differentiated with 1% acid alcohol and stained with eosin Y solution for 2 min [24]. After dehydration through increasing concentrations of ethanol and clearing in xylene, the sections were mounted with neutral resin [44]. Morphological structures and pathological alterations were observed and captured using an inverted microscope (Olympus, Tokyo, Japan).

### 2.8. Immunohistochemistry

Brain tissues were fixed in 4% paraformaldehyde, embedded in paraffin, and coronally sectioned at a thickness of 5 µm. For IHC staining, sections were deparaffinized in xylene and rehydrated through a graded ethanol series. Antigen retrieval was performed by heating sections in a citrate buffer (pH 6.0) at 95 °C for 15 min [45]. To eliminate endogenous

peroxidase activity, sections were incubated with 3% $H_2O_2$ for 10 min at room temperature. After blocking with 5% normal goat serum for 1 h to minimize non-specific binding, sections were incubated overnight at 4 °C with a rabbit anti-TH primary antibody (Santa Cruz, CA, USA; 1:200 dilution). Following three washes with PBS, the sections were incubated with a biotinylated secondary antibody for 30 min at 37 °C [46]. Visualization was achieved using a 3,3′-diaminobenzidine (DAB) substrate kit, and the nuclei were counterstained with hematoxylin.

To assess TH expression in the STR, brain sections were incubated with anti-TH primary antibody overnight at 4 °C, followed by secondary antibody at 37 °C for 30 min. Visualization was performed using a DAB kit, and sections were counterstained with hematoxylin [47]. TH-positive staining was imaged, and mean optical density was quantified using Fiji v2.9 (National Institutes of Health, Bethesda, MD, USA).

### *2.9. Gut Microbiota Analysis*

Total genomic DNA was extracted using HiPure Stool DNA Kits (Magen, Guangzhou, China). The V3–V4 regions of the 16S rRNA gene were amplified with primers 341F and 806R and sequenced on the Illumina Novaseq 6000 platform (2 × 250 bp) [31]. Raw reads were quality-filtered using FASTP (v0.18.0) and merged into tags via FLASH (v1.2.11). Operational taxonomic units (OTUs) were clustered at 97% similarity using the Uparse (v9.2.64) pipeline, with chimeras removed by UCHIME [48]. Taxonomic assignment was performed against the SILVA database (v138) using the RDP Classifier (v2.2). Alpha and Beta diversity (PCoA based on UniFrac distances) were calculated via QIIME (v1.9.1). Significantly different taxa were identified using LEfSe analysis (LDA score > 3.0) [49]. Data were submitted to the NCBI BioProject database on 29 December 2025 (Accession No. PRJNA1394776).

### *2.10. Statistical Analysis*

Data were presented as mean ± SEM, with the number of replicates ($n$) indicated in the corresponding figure legends. The normality of data distribution was assessed using the Shapiro–Wilk test, and the homogeneity of variances was confirmed by Levene's test. Furthermore, differences between groups were evaluated using one-way ANOVA followed by the Student-Newman-Keuls (SNK) post hoc test, which offers appropriate sensitivity for detecting graded intergroup differences under conditions of equal sample size and homogeneous variance. A $p$-value < 0.05 was considered statistically significant. Statistical analysis was performed using IBM SPSS Statistics 25.0 (IBM, Armonk, NY, USA) and GraphPad Prism 8.0 (GraphPad Software, San Diego, CA, USA).

## 3. Results

### *3.1. Effect of LMWF on Anxiety and Hyperactive Behavior*

Rodents typically exhibit thigmotaxis, preferring to remain close to the walls and avoid the center of the arena due to innate anxiety. In contrast, SHR, as the well-established ADHD model, display hyperlocomotion, increased central zone entries, and elevated stretch behavior, which are commonly associated with hyperactivity and impulsivity (Mod group, Figure 1).

Compared to the Mod group, both ATO and LMWF treatments significantly reduced locomotor activity, as reflected by decreased total movement distance (Figure 1B). In addition, changes were observed in central zone exploration (Figure 1C) and stretch frequency (Figure 1D). Animals in the LMWFL and Pos groups exhibited movement profiles comparable to those of the Con group, indicating a substantial normalization of hyperactivity-related behaviors. Representative movement trajectories are illustrated in Figure 1E.

These finding indicate that LMWF effectively attenuated hyperactivity-related behaviors in SHR. Alterations in central zone exploration may suggest a potential influence on anxiety-like behavior. Low-dose LMWF demonstrated comparable efficacy to ATO, highlighting its potential as a non-stimulant candidate for improving ADHD-related behavioral abnormalities.

### *3.2. Effect of LMWF on Spatial Learning and Memory*

The MWM test was conducted to evaluate the impact of LMWF on spatial learning and memory. During positional navigation, escape latency was primarily influenced by the distance from the entry point to the platform (Figure 2A).

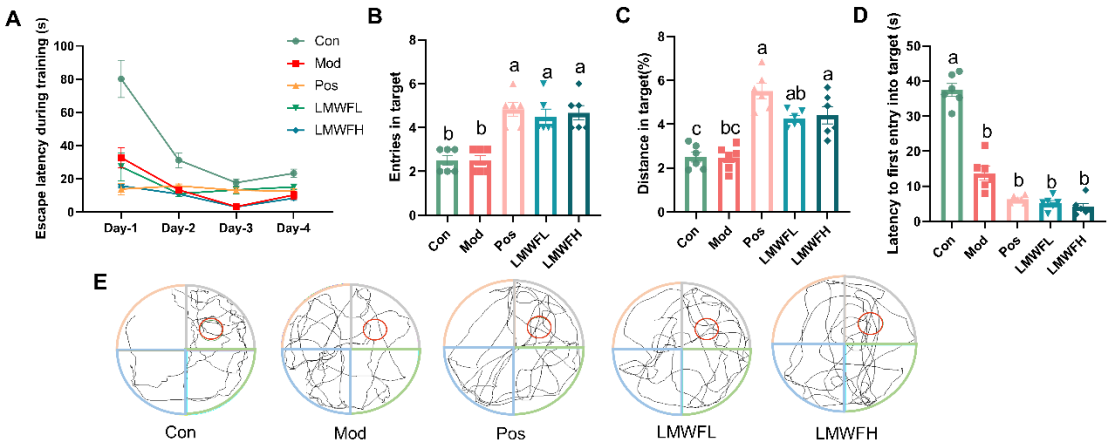


**Figure 2.** Regulation of LMWF on the spatial memory and learning ability of animals assessed by the Morris Water Maze test. (**A**) Escape latency during the position navigation (in the position navigation). (**B**) Number of entries into target in the spatial navigation. (**C**) Percentage of distance traveled in the target in the spatial navigation. (**D**) Latency to first entry into target (in the spatial navigation). (**E**) Representative swimming trajectories of each group in the spatial navigation. Data are presented as mean ± SEM ($n \geq 6$). Groups sharing the same letter are not significantly different, while groups labeled different letters differ significantly ($p < 0.05$). The red circle indicates the location of the hidden escape platform in quadrant III. WKY, Wistar-Kyoto rats; SHR, spontaneously hypertensive rats; ATO, atomoxetine; LMWF, low molecular weight fucoidan; Con, the control group of WKY animals; Mod, the model group of SHR animals without treatment; Pos, the positive group of SHR animals with ATO treatment; LMWFL, the group of SHR animals with 100 mg/kg/day LMWF treatment; LMWFH, the group of SHR animals with 300 mg/kg/day LMWF treatment.

In the spatial exploration test, animals in Mod group exhibited disoriented swimming patterns and reduced focus on the target quadrant. In contrast, animals treated with ATO and LMWF showed significantly increased entries into the original platform location (Figure 2B), greater cumulative movement distance in the target zone (Figure 2C), and reduced latency to reach this area (Figure 2D). These behavioral patterns indicate that memory retrieval and spatial navigation were preserved. Representative swimming paths are presented in Figure 2E. Collectively, these results demonstrate that LMWF enhances spatial memory performance in SHR rats.

Although WKY rats are traditionally used as controls, their hypoactivity and pronounced floating behavior compromised in the interpretability of their MWM performance, consistent with previous reports [24].

### 3.3. Regulation of Dopaminergic System by LMWF

Dopaminergic dysregulation in the prefrontal cortex (PFC) [50] and striatum (STR) [51] is a central hypothesis in the pathophysiology of ADHD, given their pivotal roles in cognitive control, working memory, and reward processing.

Liquid chromatography-mass spectrometry (LC-MS) revealed that DA levels were significantly reduced in the PFC of model animals, while LMWF treatment robustly restored DA concentrations (Figure 3A). In the STR, both LMWF and ATO significantly elevated DA levels (Figure 3B), suggesting region-specific effects on dopaminergic tone.

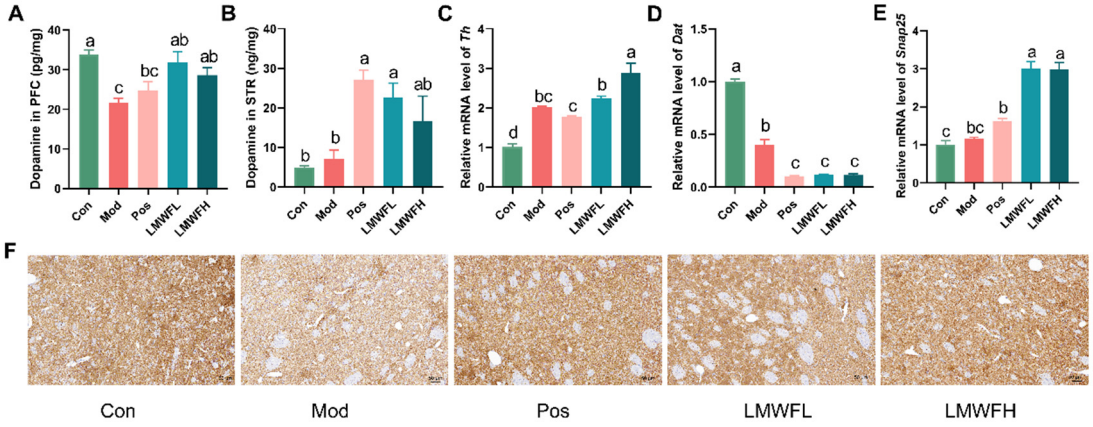


**Figure 3.** Regulatory effects of LMWF on the dopaminergic system. (**A**,**B**) Dopamine levels in the PFC and STR, respectively. (**C**–**E**) Relative mRNA expression levels of *Th*, *Dat*, and *Snap25*. (**F**) Protein expression levels of TH in the STR, respectively. Data are presented as mean ± SEM ($n \geq 6$). Groups sharing the same letter are not significantly different, whereas groups labeled with different letters differ significantly ($p < 0.05$). PFC, prefrontal cortex; STR, striatum; *Th*/TH tyrosine hydroxylase; *Dat*, dopamine transporter; *Snap25*, synaptosome-associated protein-25; WKY, Wistar-Kyoto rats; SHR, spontaneously hypertensive rats; ATO, atomoxetine; LMWF, low molecular weight fucoidan; Con, the control group of WKY animals; Mod, the model group of SHR animals without treatment; Pos, the positive group of SHR animals with ATO treatment; LMWFL, the group of SHR animals with 100 mg/kg/day LMWF treatment; LMWFH, the group of SHR animals with 300 mg/kg/day LMWF treatment.

To explore underlying the underlying mechanisms, transcriptional and protein expression analyses of key regulatory factors were conducted. LMWF significantly upregulated *Th*, the rate-limiting enzyme in DA biosynthesis (Figure 3C). Consistently, TH protein expression in the STR was also increased following LMWF treatment (Figure 3F). Concurrently, both LMWF and ATO downregulated *Dat* expression (Figure 3D), which may be associated with altered dopamine transport dynamics. LMWF markedly increased *Snap25* mRNA levels (Figure 3E), suggesting potential involvement in synaptic function.

These results suggest that LMWF is associated with multi-level modulation of dopaminergic signaling, including *Th*, *Dat* and *Snap25* expression. These coordinated alterations may contribute to the observed improvements in behavioral performance.

### 3.4. Effect of LMWF on Neurotransmitter Levels in the PFC

Although the etiology of ADHD is not fully elucidated, prevailing hypotheses highlight disruptions in monoaminergic systems, particularly dopaminergic (DA), noradrenergic (NE), and serotonergic (5-HT) pathways [52–54], as key contributors. Recent studies also implicate imbalances in excitatory and inhibitory neurotransmission, involving glutamate (Glu), $\gamma$-aminobutyric acid (GABA), glycine (Gly), and the acetylcholine (ACh) system, along with emerging molecular regulators such as GIT1 and related kinases [55–57].

LMWF significantly elevated NE concentrations (Figure 4A), indicating its capacity to restore noradrenergic tone, potentially contributing to enhanced attention and arousal regulation [54]. Both LMWF and ATO significantly reduced tyrosine (Tyr) levels (Figure 4B), which may be associated with changes in dopaminergic activity. In parallel, LMWF and ATO significantly reduced the levels of homovanillic acid (HVA), a DA metabolite (Figure 4C), suggesting alterations in dopamine metabolism.

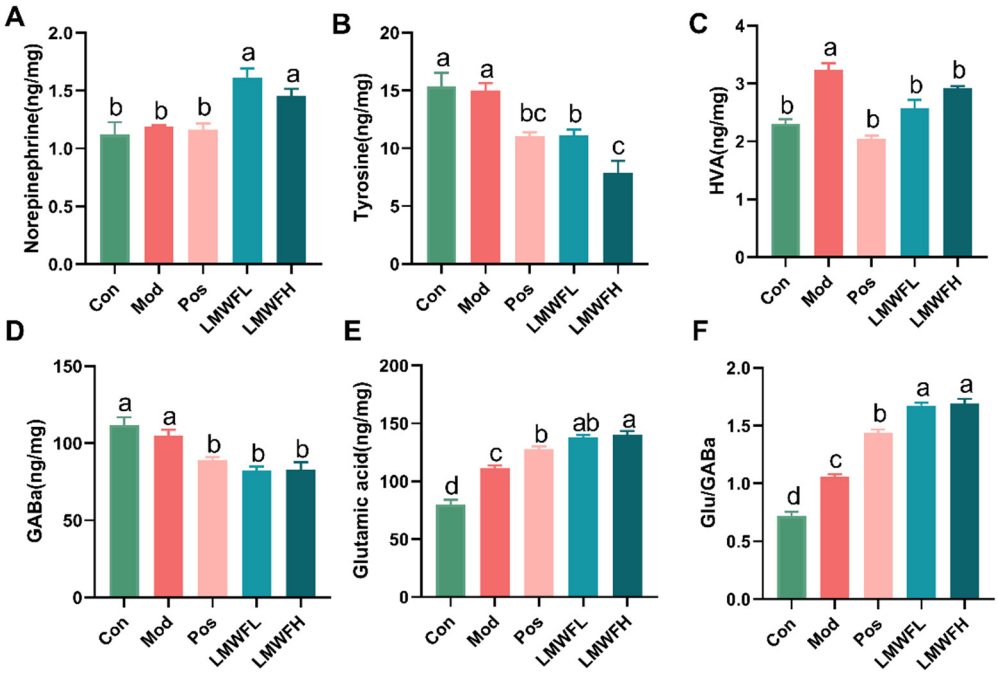


**Figure 4.** Effects of LMWF on neurotransmitter levels in the PFC. (**A**) Norepinephrine, (**B**) Tyrosine, (**C**) HVA, (**D**) GABA, (**E**) Glutamic acid, (**F**) Glutamate/GABA ratio. Data are presented as mean ± SEM ($n \geq 6$). Groups sharing the same letter are not significantly different, whereas groups labeled with different letters differ significantly ($p < 0.05$). HVA, Homovanillic acid; GABA, $\gamma$-Aminobutyric acid; Glu, glutamic acid; WKY, Wistar-Kyoto rats; SHR, spontaneously hypertensive rats; ATO, atomoxetine; LMWF, low molecular weight fucoidan; Con, the control group of WKY animals; Mod, the model group of SHR animals without treatment; Pos, the positive group of SHR animals with ATO treatment; LMWFL, the group of SHR animals with 100 mg/kg/day LMWF treatment; LMWFH, the group of SHR animals with 300 mg/kg/day LMWF treatment.

Inhibitory and excitatory neurotransmitter profiles revealed further insights into LMWF's neuromodulatory effects. After LMWF administration, GABA levels were increased (Figure 4D) and Glu levels were reduced (Figure 4E) compared with the Mod group, indicating a shift in excitatory/inhibitory balance. LMWF treatment partially restored this balance (Figure 4F), which may be associated with improved neural function [55].

These results align with the hypothesis that DA deficiency contributes to cortical hypoexcitability and impaired top-down regulation in ADHD [58]. By simultaneously enhancing DA and NE levels while modulating Glu and GABA balance, LMWF was associated with coordinated changes in multiple neurotransmitter systems. The reduction in HVA levels, combined with increased DA and NE, further underscores improved monoaminergic efficiency, potentially ameliorating cognitive and behavioral symptoms.

Together, these findings suggest that LMWF is associated with modulation of monoaminergic signaling and excitatory/inhibitory balance in the ADHD model, which may contribute to improvements in cognitive and behavioral functions.

### *3.5. Histopathological Alterations*

In SHR model rats, neuronal cells exhibited pronounced morphological damage, including disordered architecture, cellular dispersion, nuclear shrinkage, and signs of apoptosis such as pyknosis, disrupted nuclear membranes, and nucleolar loss (Figure 5A, blue circle). Following LMWF administration, these histopathological features appeared less pronounced.

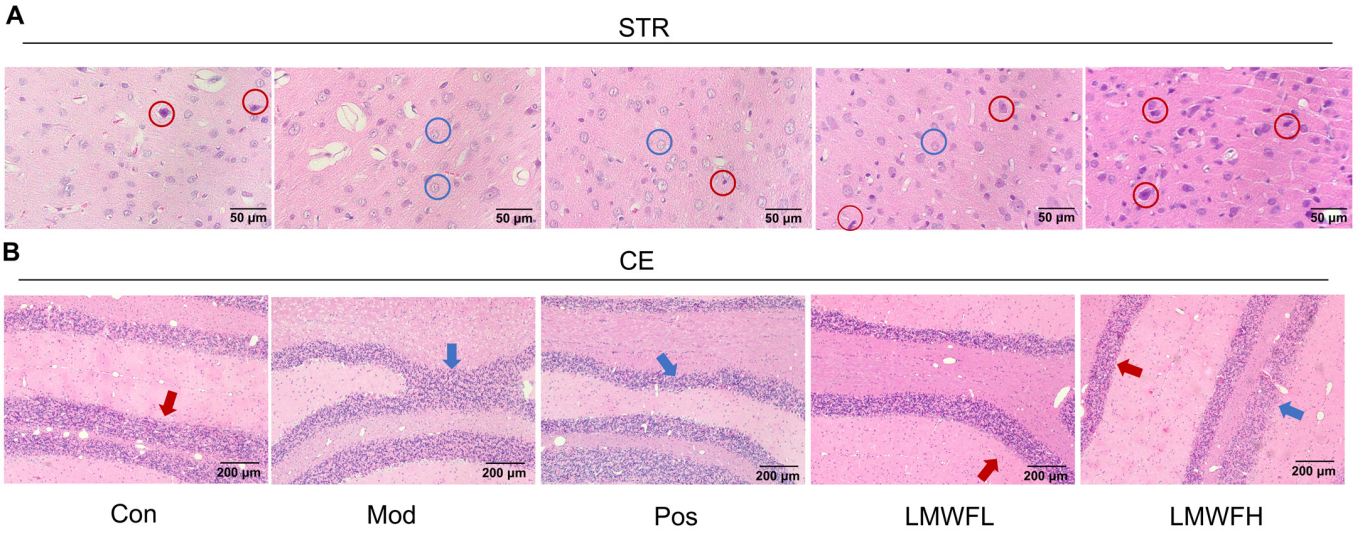


**Figure 5.** Histopathological analysis of the striatum (STR) (**A**) and cerebral cortex (CE) (**B**). Red circles indicate pyknotic neurons, characterized by hyperchromatic nuclei and cytoplasmic condensation. Blue arrows indicate ruptured nuclear membranes and absence of nucleoli. Images are representative of $n = 3$ animals per group. Scale bars: 50 μm (**upper panels**), 200 μm (**lower panels**). The blue circle indicates neuronal damage area; the red circle indicates the region with preserved neuronal morphology. The blue arrow indicates a disorganized granular layer; the red arrow indicates an intact granular layer. STR, striatum; CE, cerebellum; WKY, Wistar-Kyoto rats; SHR, spontaneously hypertensive rats; ATO, atomoxetine; LMWF, low molecular weight fucoidan; Con, the control group of WKY animals; Mod, the model group of SHR animals without treatment; Pos, the positive group of SHR animals with ATO treatment; LMWFL, the group of SHR animals with 100 mg/kg/day LMWF treatment; LMWFH, the group of SHR animals with 300 mg/kg/day LMWF treatment.

These pathological changes were markedly ameliorated by LMWF administration. Neuronal morphology in the treated groups showed relatively preserved nuclear and cytoplasmic structures and a more organized cellular arrangement (Figure 5A, red circle). These observations suggest that LMWF may alleviate histopathological alterations in SHR rats.

In the cerebellum, the untreated model group exhibited a thinner and less organized granular layer compared with controls (Figure 5B, blue arrow). After LMWF treatment, the granular layer appeared relatively more compact and structurally organized (Figure 5B, red arrow).

Collectively, H&E staining revealed that SHR rats exhibited clear signs of neuronal injury, which were significantly reversed by LMWF. In contrast, ATO did not show observable neuroprotective effects at the histological level, which may be attributable to its known gastrointestinal and systemic side effects. The restorative impact of LMWF highlights its multifaceted therapeutic potential as a natural macromolecular agent, likely operating via multiple neuroprotective pathways.

### *3.6. Gut Microbiota*

Accumulating evidence has demonstrated that natural polysaccharides exert beneficial effects on obesity, cardiovascular, cerebrovascular, and neurodegenerative diseases through

modulation of gut microbiota [59,60]. Given the increasing recognition of the brain–gut axis and the presence of inflammatory features in ADHD pathology, this study evaluated the regulatory effect of LMWF on the gut microbiota.

At the family level (Figure 6A), LMWF treatment significantly increased the abundance of *Lactobacillaceae*, *Bacteroidaceae*, and *Prevotellaceae*, while reducing the levels of *Muribaculaceae*, *Lachnospiraceae*, *Erysipelotrichaceae*, *Saccharimonadaceae*, and *Desulfovibrionaceae*. Among these, *Lactobacillaceae* and *Bacteroidaceae* are known short-chain fatty acid (SCFA) producers, which contribute to maintaining intestinal homeostasis and reducing systemic inflammation [61]. Consistently, the abundance profiles of these key bacterial families in the LMWF-treated group resembled those of healthy controls. *Desulfovibrionaceae*, a family of sulfate-reducing bacteria capable of producing cytotoxic $H_2S$, was significantly reduced by LMWF, indicating improved intestinal epithelial barrier function.

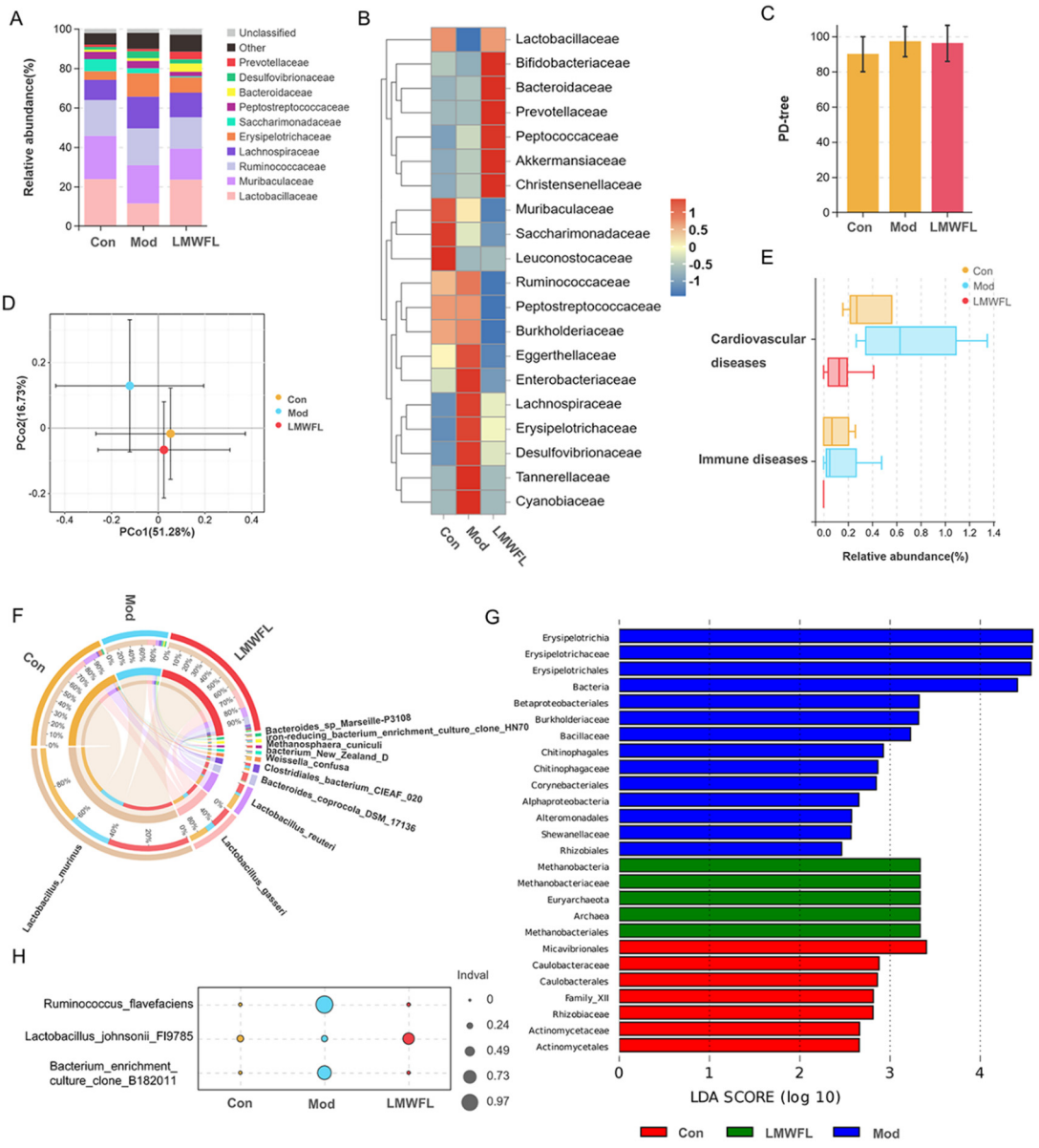


**Figure 6.** Regulatory effect of LMWF on gut microbiota. (**A**) Stacked bar plot showing species distribution at the family level. (**B**) Heatmap of species abundance at the family level. (**C**) $\alpha$-diversity analysis of microbial communities. (**D**) $\beta$-diversity analysis based on principal coordinates analysis (PCoA). (**E**) Functional prediction using PICRUSt2 and Kruskal–Wallis rank-sum test. (**F**) Circos

plot illustrating the distribution and abundance of species-level taxa. (**G**) LEfSe analysis identifying differential taxa at the family level. (**H**) Indicator species analysis at the species level. Statistical analysis and taxonomic profiling were performed with $n = 3$ animals per group. WKY, Wistar-Kyoto rats; SHR, spontaneously hypertensive rats; LMWF, low molecular weight fucoidan; Con, the control group of WKY animals; Mod, the model group of SHR animals without treatment; LMWFL, the group of SHR animals with 100 mg/kg/day LMWF treatment.

Figure 6B further illustrates species-level alterations, where LMWF upregulated beneficial taxa including *Akkermansiaceae*, *Bifidobacteriaceae*, and *Christensenellaceae*, while reducing pro-inflammatory or dysbiosis-associated families such as *Burkholderiaceae*, *Eggerthellaceae*, and *Enterobacteriaceae*. *Akkermansia muciniphila*, a key member of *Akkermansiaceae*, is recognized for its role in enhancing mucosal integrity and exerting anti-inflammatory effects [5,6]. Its decreased abundance has been associated with metabolic and neurodegenerative diseases, while supplementation has been shown to alleviate cognitive decline and amyloid pathology in Alzheimer's disease models. *Christensenellaceae*, negatively correlated with systemic inflammation, has also been implicated in host metabolic health and longevity [62].

In terms of diversity, $\alpha$-diversity analysis showed no significant difference between groups, indicating comparable overall richness (Figure 6C). However, $\beta$-diversity analysis revealed significant shifts in microbial community composition between the Mod and LMWF-treated groups (Figure 6D), suggesting that LMWF altered the structural landscape of the gut microbiota.

Functional prediction based on KEGG pathway enrichment (Figure 6E) revealed that LMWF significantly downregulated microbiota functions associated with cardiovascular and autoimmune diseases. These findings indicate a shift towards a more health-associated microbial metabolic profile, potentially contributing to neuroimmune regulation and behavioral improvement through the gut–brain axis.

Species-level comparison via Circos plot (Figure 6F) identified increased abundance of *Lactobacillus murinus*, *L. gasseri*, and *L. reuteri* in the LMWF-treated group. These species are known to modulate immune responses, regulate excitatory/inhibitory neurotransmitter balance, and enhance intestinal health via SCFA production [63]. LefSe analysis further identified *Erysipelotrichia* and its associated taxonomic levels (*Erysipelotrichaceae*, *Erysipelotrichales*) as prominent biomarkers of the Mod group (Figure 6G), suggesting their potential role in ADHD-associated gut dysbiosis.

Indicator species analysis (Figure 6H) showed that *Ruminococcus flavefaciens* and *Bacterium enrichment culture clone B182011* were elevated in the Mod group, both of which have been implicated in intestinal barrier disruption and inflammation. Conversely, *Lactobacillus johnsonii* was markedly enriched in the LMWF group, supporting its beneficial regulatory role.

In conclusion, LMWF effectively modulates gut microbial composition and function by enriching beneficial taxa involved in immune and neuronal regulation, while suppressing pathogenic bacteria associated with inflammation and neurotoxicity. These findings support the hypothesis that LMWF may exert neuroprotective effects, at least in part, via modulation of the gut microbiota along the brain–gut axis.

## 4. Discussion

The present study highlights the therapeutic potential of LMWF in mitigating ADHD-like phenotypes, including hyperactivity and cognitive impairment, in the SHR model. The behavioral deficits in SHR rats are resulting from compromised DA signaling in PFC and STR. In alignment with the findings of Wang et al., LMWF administration effectively restored DA homeostasis in critical brain regions. This evidenced by the reduction in locomotive distance and stretching frequency in the central zone of the open field test, which metrics indicative of attenuated anxiety and hyperactivity [64].

Distinguished from the clinical stimulant ATO, LMWF as a marine-derived bioactive polysaccharide, exhibits a superior safety profile and minimal toxicity, positioning it as a promising non-stimulant candidate for intervention. Mechanistic evaluation reveals that LMWF may modulate multiple components of dopaminergic signaling. LMWF augments DA biosynthesis by upregulating *Th* expression, facilitates synaptic vesicle trafficking via *Snap25* elevation, and modulates synaptic DA availability by downregulating *Dat*. This coordinated action contributes to the maintenance of neurotransmitter equilibrium within the PFC and STR [65].

Furthermore, LMWF conferred significant neuroprotection, as demonstrated by the preserved neuronal architecture in the STR and cerebellum, which reinforces its potential for long-term therapeutic application. From the perspective of the gut-brain axis, LMWF functions as a potent prebiotic-like modulator, remodeling the commensal landscape by significantly enriching beneficial taxa such as *Akkermansia* and SCFA-producing *Lactobacillus*. These microbial shifts are instrumental in reinforcing intestinal barrier integrity and suppressing systemic neuroinflammation [60,61].

The neuroprotective efficacy of LMWF observed in this study aligns with the emerging role of natural polysaccharides as therapeutic interventions for neurological disorders. Consistent with previous reports on *Schisandra chinensis* polysaccharides [35,66] and *Sea buckthorn* polysaccharides [67], LMWF effectively modulated the neurochemical environment and ameliorated cognitive deficits. LMWF's role in reshaping gut microbiota to improve ADHD-like behaviors parallels the mechanism of *Dendrobium officinale* polysaccharide [68] and *Schisandra chinensis* polysaccharides [35], which attenuates cognitive impairment via the gut-brain axis. From a structure-activity perspective, the bioactivity of LMWF is likely supported by its low molecular weight and high degree of sulfation, which may facilitate its systemic influence on neurochemical and microbial homeostasis [28,59]. Collectively, these findings suggest that LMWF may serves as a potent dietary intervention for ADHD-like symptoms, possibly involving coordinated modulation of multiple biological pathways.

Despite these insights, the precise structure-activity relationship, particularly how sulfation patterns influence receptor binding, remains to be elucidated. Integrating metabolomics to quantify microbial-derived metabolites would provide a more granular understanding of gut-brain signaling. Nevertheless, this study provides a robust scientific foundation for utilizing LMWF as a promising functional food intervention for ADHD.

## 5. Limitations

This study has several limitations that should be acknowledged. Although the SHR is a widely accepted model for ADHD-like behavior, its hyperactive phenotype primarily reflects the locomotor dimension of the disorder. In this study, behavioral assessments were limited to the open field test and the Morris water maze, which capture locomotor activity, anxiety-like behavior, and spatial learning and memory, respectively. However, neither task directly measures sustained attention or impulsive responding—two core symptom domains of ADHD. The use of attention-specific paradigms such as the five-choice serial reaction time task (5-CSRTT) or delay discounting tasks would be required to evaluate these aspects.

Moreover, dopaminergic regulation was inferred from neurotransmitter levels measured by LC-MS/MS and mRNA expression of three key genes (Th, Dat, and Snap25) quantified by qRT-PCR in the prefrontal cortex. Although these markers provide valuable information, they do not directly reflect dopamine synthesis rates, vesicular storage, synaptic release, reuptake kinetics, or receptor occupancy. In vivo micro-dialysis, voltammetry, or PET imaging would be necessary to capture dynamic dopaminergic function. Moreover, protein-level confirmation of DAT and SNAP25 expression was not performed, which

warrants cautious interpretation of the transcriptional findings. Furthermore, although alterations in gut microbiota composition were observed, no direct measurements of inflammatory markers, intestinal permeability, or neuroimmune signaling were performed, limiting the mechanistic interpretation of gut–brain interactions. Future studies incorporating functional assays and multi-level validation are therefore required to further elucidate the underlying mechanisms.

## 6. Conclusions

This study demonstrates that LMWF exerts beneficial effects on ADHD-like phenotypes in SHR. Behaviorally, LMWF ameliorated hyperactivity-related parameters and improved performance in cognitive tasks. At the neurochemical level, LMWF was associated with alterations in dopaminergic signaling, including increased dopamine levels and changes in the expression of key regulatory factors such as *Th*, *Dat*, and *Snap25*. These findings suggest a potential involvement of dopaminergic pathways, although direct mechanistic relationships remain to be further elucidated. In addition, histological observations indicated that LMWF treatment was associated with improved neuronal morphology in the striatum and cerebellum. Furthermore, LMWF was found to modulate gut microbiota composition, which may contribute to its overall effects through gut–brain interactions. Taken together, these results suggest that LMWF exerts multi-level regulatory effects involving behavioral, neurochemical, and microbiota-related changes. While the underlying mechanisms require further investigation, LMWF may represent a promising candidate for dietary intervention in ADHD-related conditions.

**Author Contributions:** Y.L.: Investigation, Formal analysis, Methodology, Data curation, Visualization, Writing—original draft; J.W.: Methodology, Validation, Funding acquisition; N.W.: Methodology, Validation; Y.Y.: Methodology, Validation; L.G.: Methodology, Validation, Funding acquisition; Q.Z.: Methodology, Project administration, Funding acquisition, Supervision, Writing—review & editing. All authors have read and agreed to the published version of the manuscript.

**Funding:** This work was financially supported by the Key Technology Breakthrough and Industrialization Demonstration Projects of Qingdao City (Grant No. 26-1-1-gjgg-58-nsh), and the Science and Technology Service Network Initiative Program Supporting Project of Fujian Province (Grant No. 2023T3057).

**Institutional Review Board Statement:** All animal procedures were carried out in accordance with the Guidelines for the Care and Use of Laboratory Animals issued by the Ministry of Health of the People's Republic of China (Documentation No. 55, 2001), and adhered to internationally accepted principles for the ethical use of laboratory animals. The experimental protocol was reviewed and approved by the Animal Ethics Committee of Qingdao University (Approval No. 20211126SHR10020220115006) on 21 October 2021.

**Informed Consent Statement:** Not applicable.

**Data Availability Statement:** The raw data supporting the conclusions of this article will be made available by the authors, without undue reservation. The 16S rRNA gene sequencing data generated during this study have been deposited in the National Center for Biotechnology Information (NCBI) BioProject database under the accession number PRJNA1394776. Other datasets analyzed during the current study are available from the corresponding author on reasonable request.

**Acknowledgments:** I sincerely thank all the team members who assisted me with the animal experiments and my supervisor for their unreserved guidance and support. Thanks to Reward and Home for Researchers (www.home-for-researchers.com) for their support.

**Conflicts of Interest:** The authors declare that there are no conflicts of interest.

## References


1. Valladão, S.C.; França, A.P.; Pandolfo, P.; Dos Santos-Rodrigues, A. Adenosinergic system and nucleoside transporters in attention deficit hyperactivity disorder: Current findings. *Neurosci. Biobehav. Rev.* **2024**, *164*, 105771. [CrossRef]
2. Li, F.; Cui, Y.; Li, Y.; Guo, L.; Ke, X.; Liu, J.; Luo, X.; Zheng, Y.; Leckman, J.F. Prevalence of mental disorders in school children and adolescents in China: Diagnostic data from detailed clinical assessments of 17,524 individuals. *J. Child Psychol. Psychiatry* **2022**, *63*, 34–46. [CrossRef]
3. Carlsson, T.; Molander, F.; Taylor, M.J.; Jonsson, U.; Bölte, S. Early environmental risk factors for neurodevelopmental disorders—A systematic review of twin and sibling studies. *Dev. Psychopathol.* **2021**, *33*, 1448–1495. [CrossRef]
4. Wetherill, L.; Foroud, T.; Goodlett, C. Meta-Analyses of Externalizing Disorders: Genetics or Prenatal Alcohol Exposure? *Alcohol. Clin. Exp. Res.* **2018**, *42*, 162–172. [CrossRef] [PubMed]
5. Song, P.; Zha, M.; Yang, Q.; Zhang, Y.; Li, X.; Rudan, I. The prevalence of adult attention-deficit hyperactivity disorder: A global systematic review and meta-analysis. *J. Glob. Health* **2021**, *11*, 04009. [CrossRef]
6. Yates, J.R. Aberrant glutamatergic systems underlying impulsive behaviors: Insights from clinical and preclinical research. *Prog. Neuro-Psychopharmacol. Biol. Psychiatry* **2024**, *135*, 111107. [CrossRef]
7. Olsen, D.; Wellner, N.; Kaas, M.; de Jong, I.E.M.; Sotty, F.; Didriksen, M.; Glerup, S.; Nykjaer, A. Altered dopaminergic firing pattern and novelty response underlie ADHD-like behavior of SorCS2-deficient mice. *Transl. Psychiatry* **2021**, *11*, 74. [CrossRef] [PubMed]
8. Leng, Y.; Wu, N.; Wang, J.; Geng, L.; Yue, Y.; Zhang, Q. Astaxanthin Mitigates ADHD Symptoms in Spontaneously Hypertensive Rats via Dopaminergic Modulation and Brain–Gut Axis Regulation. *Molecules* **2025**, *30*, 1637. [CrossRef]
9. Franke, B.; Vasquez, A.A.; Johansson, S.; Hoogman, M.; Romanos, J.; Boreatti-Hümmer, A.; Heine, M.; Jacob, C.P.; Lesch, K.-P.; Casas, M.; et al. Multicenter Analysis of the SLC6A3/DAT1 VNTR Haplotype in Persistent ADHD Suggests Differential Involvement of the Gene in Childhood and Persistent ADHD. *Neuropsychopharmacology* **2010**, *35*, 656–664. [CrossRef] [PubMed]
10. Rovira, P.; Demontis, D.; Sánchez-Mora, C.; Zayats, T.; Klein, M.; Mota, N.R.; Weber, H.; Garcia-Martínez, I.; Pagerols, M.; Vilar-Ribó, L.; et al. Shared genetic background between children and adults with attention deficit/hyperactivity disorder. *Neuropsychopharmacology* **2020**, *45*, 1617–1626. [CrossRef]
11. Darwish, A.H.; Elgohary, T.M.; Nosair, N.A. Serum Interleukin-6 Level in Children With Attention-Deficit Hyperactivity Disorder (ADHD). *J. Child Neurol.* **2019**, *34*, 61–67. [CrossRef] [PubMed]
12. Wu, N.; Li, Z.; Wang, J.; Geng, L.; Yue, Y.; Deng, Z.; Wang, Q.; Zhang, Q. Low molecular weight fucoidan attenuating pulmonary fibrosis by relieving inflammatory reaction and progression of epithelial-mesenchymal transition. *Carbohydr. Polym.* **2021**, *273*, 118567. [CrossRef]
13. Li, Z.; Wu, N.; Wang, J.; Yue, Y.; Geng, L.; Zhang, Q. Low molecular weight fucoidan alleviates cerebrovascular damage by promoting angiogenesis in type 2 diabetes mice. *Int. J. Biol. Macromol.* **2022**, *217*, 345–355. [CrossRef]
14. Deng, Z.; Wu, N.; Wang, J.; Geng, L.; Yue, Y.; Wang, F.; Zhang, Q. Low molecular weight fucoidan fraction LF2 improves metabolic syndrome via up-regulating PI3K-AKT-mTOR axis and increasing the abundance of *Akkermansia muciniphila* in the gut microbiota. *Int. J. Biol. Macromol.* **2021**, *193*, 789–798. [CrossRef] [PubMed]
15. Wang, J.; Liu, H.; Jin, W.; Zhang, H.; Zhang, Q. Structure–activity relationship of sulfated hetero/galactofucan polysaccharides on dopaminergic neuron. *Int. J. Biol. Macromol.* **2016**, *82*, 878–883. [CrossRef] [PubMed]
16. Wang, J.; Liu, H.; Zhang, X.; Li, X.; Geng, L.; Zhang, H.; Zhang, Q. Sulfated Hetero-Polysaccharides Protect SH-SY5Y Cells from $H_2O_2$-Induced Apoptosis by Affecting the PI3K/Akt Signaling Pathway. *Mar. Drugs* **2017**, *15*, 110. [CrossRef]
17. Regan, S.L.; Williams, M.T.; Vorhees, C.V. Review of rodent models of attention deficit hyperactivity disorder. *Neurosci. Biobehav. Rev.* **2022**, *132*, 621–637. [CrossRef]
18. Sagvolden, T.; Metzger, M.A.; Schiorbeck, H.K.; Rugland, A.-L.; Spinnangr, I.; Sagvolden, G. The spontaneously hypertensive rat (SHR) as an animal model of childhood hyperactivity (ADHD): Changed reactivity to reinforcers and to psychomotor stimulants. *Behav. Neural Biol.* **1992**, *58*, 103–112. [CrossRef]
19. Luo, Z.; Pang, S.; Zhang, L. Research progress on genetic models of common mental disorders in rats and mice. *Chin. J. Comp. Med.* **2021**, *31*, 119–126.
20. Grauer, E.; Kapon, Y. Wistar-Kyoto rats in the Morris water maze: Impaired working memory and hyper-reactivity to stress. *Behav. Brain Res.* **1993**, *59*, 147–151. [CrossRef]
21. Sagvolden, T. Behavioral validation of the spontaneously hypertensive rat (SHR) as an animal model of attention-deficit/hyperactivity disorder (AD/HD). *Neurosci. Biobehav. Rev.* **2000**, *24*, 31–39. [CrossRef]
22. van der Kooij, M.A.; Glennon, J.C. Animal models concerning the role of dopamine in attention-deficit hyperactivity disorder. *Neurosci. Biobehav. Rev.* **2007**, *31*, 597–618. [CrossRef]
23. Sagvolden, T.; Russell, V.A.; Aase, H.; Johansen, E.B.; Farshbaf, M. Rodent models of attention-deficit/hyperactivity disorder. *Biol. Psychiatry* **2005**, *57*, 1239–1247. [CrossRef] [PubMed]

24. Yuan, H.; Ni, X.; Zheng, M.; Han, X.; Song, Y.; Yu, M. Effect of catalpol on behavior and neurodevelopment in an ADHD rat model. *Biomed. Pharmacother.* **2019**, *118*, 109033. [CrossRef]
25. Xia, W.-J.; Xu, M.-L.; Yu, X.-J.; Du, M.-M.; Li, X.-H.; Yang, T.; Li, L.; Li, Y.; Kang, K.B.; Su, Q.; et al. Antihypertensive effects of exercise involve reshaping of gut microbiota and improvement of gut-brain axis in spontaneously hypertensive rat. *Gut Microbes* **2021**, *13*, 1–24. [CrossRef]
26. Fu, D.; Wu, D.-D.; Guo, H.-L.; Hu, Y.-H.; Xia, Y.; Ji, X.; Fang, W.-R.; Li, Y.-M.; Xu, J.; Chen, F.; et al. The Mechanism, Clinical Efficacy, Safety, and Dosage Regimen of Atomoxetine for ADHD Therapy in Children: A Narrative Review. *Front. Psychiatry* **2022**, *12*, 780921. [CrossRef] [PubMed]
27. Xing, M.; Li, G.; Liu, Y.; Yang, L.; Zhang, Y.; Zhang, Y.; Ding, J.; Lu, M.; Yu, G.; Hu, G. Fucoidan from fucus vesiculosus prevents the loss of dopaminergic neurons by alleviating mitochondrial dysfunction through targeting ATP5F1a. *Carbohydr. Polym.* **2023**, *303*, 120470. [CrossRef]
28. Yang, X.; Zhang, X.; Ma, Y.; Li, S.; Wang, Q.; Hong, J.-S.; Yu, G.; Qi, B.; Wang, J.; Liu, C.; et al. Fucoidan ameliorates rotenone-induced parkinsonism in mice by regulating the microbiota-gut-brain axis. *Int. J. Biol. Macromol.* **2024**, *283*, 137373. [CrossRef]
29. Seibenhener, M.L.; Wooten, M.C. Use of the Open Field Maze to Measure Locomotor and Anxiety-like Behavior in Mice. *J. Vis. Exp.* **2015**, 52434. [CrossRef]
30. Fang, Z.; Shen, G.; Amin, N.; Lou, C.; Wang, C.; Fang, M. Effects of neuroinflammation and autophagy on the structure of the blood-brain barrier in ADHD model. *Neuroscience* **2023**, *530*, 17–25. [CrossRef]
31. Zhang, Y.; Zhang, J.; Wu, J.; Zhu, Q.; Chen, C.; Li, Y. Implications of gut microbiota dysbiosis and fecal metabolite changes in psychologically stressed mice. *Front. Microbiol.* **2023**, *14*, 1124454. [CrossRef]
32. Papadopoulos, A.; Seguin, D.; Correa, S.; Duerden, E.G. Peer victimization and the association with hippocampal development and working memory in children with ADHD and typically-developing children. *Sci. Rep.* **2021**, *11*, 16411. [CrossRef] [PubMed]
33. Vorhees, C.V.; Williams, M.T. Morris water maze: Procedures for assessing spatial and related forms of learning and memory. *Nat. Protoc.* **2006**, *1*, 848–858. [CrossRef]
34. Liu, Q.; Zhang, J.; Xiao, C.; Su, D.; Li, L.; Yang, C.; Zhao, Z.; Jiang, W.; You, Z.; Zhou, T. Akebia saponin D protects hippocampal neurogenesis from microglia-mediated inflammation and ameliorates depressive-like behaviors and cognitive impairment in mice through the PI3K-Akt pathway. *Front. Pharmacol.* **2022**, *13*, 927419. [CrossRef]
35. Fu, J.; Li, J.; Sun, Y.; Liu, S.; Song, F.; Liu, Z. In-depth investigation of the mechanisms of *Schisandra chinensis* polysaccharide mitigating Alzheimer's disease rat via gut microbiota and feces metabolomics. *Int. J. Biol. Macromol.* **2023**, *232*, 123488. [CrossRef]
36. Kang, S.S.; Meng, L.; Zhang, X.; Wu, Z.; Mancieri, A.; Xie, B.; Liu, X.; Weinshenker, D.; Peng, J.; Zhang, Z.; et al. Tau modification by the norepinephrine metabolite DOPEGAL stimulates its pathology and propagation. *Nat. Struct. Mol. Biol.* **2022**, *29*, 292–305. [CrossRef]
37. Correia, R.; Coimbra, B.; Domingues, A.V.; Wezik, M.; Vieitas-Gaspar, N.; Gaspar, R.; Sousa, N.; Pinto, L.; Rodrigues, A.J.; Soares-Cunha, C. Involvement of nucleus accumbens D2-medium spiny neurons projecting to the ventral pallidum in anxiety-like behaviour. *J. Psychiatry Neurosci.* **2023**, *48*, E267–E284. [CrossRef]
38. Lui, J.H.; Nguyen, N.D.; Grutzner, S.M.; Darmanis, S.; Peixoto, D.; Wagner, M.J.; Allen, W.E.; Kebschull, J.M.; Richman, E.B.; Ren, J.; et al. Differential encoding in prefrontal cortex projection neuron classes across cognitive tasks. *Cell* **2021**, *184*, 489–506.e26. [CrossRef]
39. Huang, X.; Guo, X.-F.; Wang, H.; Zhang, H.-S. Analysis of catecholamines and related compounds in one whole metabolic pathway with high performance liquid chromatography based on derivatization. *Arab. J. Chem.* **2019**, *12*, 1159–1167. [CrossRef]
40. Wong, J.-M.T.; Malec, P.A.; Mabrouk, O.S.; Ro, J.; Dus, M.; Kennedy, R.T. Benzoyl chloride derivatization with liquid chromatography–mass spectrometry for targeted metabolomics of neurochemicals in biological samples. *J. Chromatogr. A* **2016**, *1446*, 78–90. [CrossRef] [PubMed]
41. Vidal, O.M.; Vélez, J.I.; Arcos-Burgos, M. ADGRL3 genomic variation implicated in neurogenesis and ADHD links functional effects to the incretin polypeptide GIP. *Sci. Rep.* **2022**, *12*, 15922. [CrossRef] [PubMed]
42. Livak, K.J.; Schmittgen, T.D. Analysis of Relative Gene Expression Data Using Real-Time Quantitative PCR and the $2^{-\Delta\Delta CT}$ Method. *Methods* **2001**, *25*, 402–408. [CrossRef]
43. Hafez, H.A.; Kamel, M.A.; Osman, M.Y.; Osman, H.M.; Elblehi, S.S.; Mahmoud, S.A. Ameliorative effects of astaxanthin on brain tissues of alzheimer's disease-like model: Cross talk between neuronal-specific microRNA-124 and related pathways. *Mol. Cell. Biochem.* **2021**, *476*, 2233–2249. [CrossRef] [PubMed]
44. Satoh, R.; Kawakami, K.; Nakadate, K. Effects of Smart Drugs on Cholinergic System and Non-Neuronal Acetylcholine in the Mouse Hippocampus: Histopathological Approach. *J. Clin. Med.* **2022**, *11*, 3310. [CrossRef]
45. Koutzoumis, D.N.; Vergara, M.; Pino, J.; Buddendorff, J.; Khoshbouei, H.; Mandel, R.J.; Torres, G.E. Alterations of the gut microbiota with antibiotics protects dopamine neuron loss and improve motor deficits in a pharmacological rodent model of parkinson's disease. *Exp. Neurol.* **2020**, *325*, 113159. [CrossRef] [PubMed]

46. Hongo, N.; Takamura, Y.; Nishimaru, H.; Matsumoto, J.; Tobe, K.; Saito, T.; Saido, T.C.; Nishijo, H. Astaxanthin Ameliorated Parvalbumin-Positive Neuron Deficits and Alzheimer's Disease-Related Pathological Progression in the Hippocampus of AppNL-G-F/NL-G-F Mice. *Front. Pharmacol.* **2020**, *11*, 307. [CrossRef]
47. Han, J.; Lee, Y.; Im, J.; Ham, Y.; Lee, H.; Han, S.; Hong, J. Astaxanthin Ameliorates Lipopolysaccharide-Induced Neuroinflammation, Oxidative Stress and Memory Dysfunction through Inactivation of the Signal Transducer and Activator of Transcription 3 Pathway. *Mar. Drugs* **2019**, *17*, 123. [CrossRef]
48. Weyns, A.-S.; Ahannach, S.; Van Rillaer, T.; De Bruyne, T.; Lebeer, S.; Hermans, N. Enhancing pediatric attention-deficit hyperactivity disorder treatment: Exploring the gut microbiota effects of french maritime pine bark extract and methylphenidate intervention. *Front. Nutr.* **2024**, *11*, 1422253. [CrossRef]
49. Zhang, W.; Guo, Y.; Cheng, Y.; Yao, W.; Qian, H. Neuroprotective effects of polysaccharide from Sparassis crispa on Alzheimer's disease-like mice: Involvement of microbiota-gut-brain axis. *Int. J. Biol. Macromol.* **2023**, *225*, 974–986. [CrossRef]
50. Sullivan, R.M.; Brake, W.G. What the rodent prefrontal cortex can teach us about attention-deficit/hyperactivity disorder: The critical role of early developmental events on prefrontal function. *Behav. Brain Res.* **2003**, *146*, 43–55. [CrossRef]
51. Russell, V.; de Villiers, A.; Sagvolden, T.; Lamm, M.; Taljaard, J. Altered dopaminergic function in the prefrontal cortex, nucleus accumbens and caudate-putamen of an animal model of attention-deficit hyperactivity disorder—The spontaneously hypertensive rat. *Brain Res.* **1995**, *676*, 343–351. [CrossRef]
52. Madhyastha, S.; Rao, M.S.; Renno, W.M. Serotonergic and adrenergic neuroreceptor manipulation ameliorates core symptoms of ADHD through modulating dopaminergic receptors in spontaneously hypertensive rats. *Int. J. Mol. Sci.* **2024**, *25*, 2300. [CrossRef]
53. Schepis, T.S.; Werner, K.S.; Figueroa, O.; McCabe, V.V.; Schulenberg, J.E.; Veliz, P.T.; Wilens, T.E.; McCabe, S.E. Type of medication therapy for ADHD and stimulant misuse during adolescence: A cross-sectional multi-cohort national study. *EClinicalMedicine* **2023**, *58*, 101902. [CrossRef]
54. Zhi, J.; Zhang, S.; Huang, M.; Qin, H.; Xu, H.; Chang, Q.; Wang, Y. Transcutaneous auricular vagus nerve stimulation as a potential therapy for attention deficit hyperactivity disorder: Modulation of the noradrenergic pathway in the prefrontal lobe. *Front. Neurosci.* **2024**, *18*, 1494272. [CrossRef]
55. Berardelli, I.; Rogante, E.; Formica, F.; Iannazzo, R.; Mammoliti, A.V.; Riccioni, R.; Veizi, S.; McIntyre, R.S.; Pompili, M. The efficacy of vortioxetine in the acute treatment of major depressive disorder: A systematic review and meta-analysis. *J. Psychopharmacol.* **2025**, *39*, 92–105. [CrossRef] [PubMed]
56. Boff, J.M.; Shrestha, A.P.; Madireddy, S.; Viswaprakash, N.; Della Santina, L.; Vaithianathan, T. The interplay between neurotransmitters and calcium dynamics in retinal synapses during development, health, and disease. *Int. J. Mol. Sci.* **2024**, *25*, 2226. [CrossRef] [PubMed]
57. Stachowicz, K. Deciphering the mechanisms of reciprocal regulation or interdependence at the cannabinoid CB1 receptors and cyclooxygenase-2 level: Effects on mood, cognitive implications, and synaptic signaling. *Neurosci. Biobehav. Rev.* **2023**, *155*, 105439. [CrossRef] [PubMed]
58. Koirala, S.; Grimsrud, G.; Mooney, M.A.; Larsen, B.; Feczko, E.; Elison, J.T.; Nelson, S.M.; Nigg, J.T.; Tervo-Clemmens, B.; Fair, D.A. Neurobiology of attention-deficit hyperactivity disorder: Historical challenges and emerging frontiers. *Nat. Rev. Neurosci.* **2024**, *25*, 759–775. [CrossRef] [PubMed]
59. Wei, B.; Zhang, B.; Du, A.-Q.; Zhou, Z.-Y.; Lu, D.-Z.; Zhu, Z.-H.; Ke, S.-Z.; Wang, S.-J.; Yu, Y.-L.; Chen, J.-W.; et al. *Saccharina japonica* fucan suppresses high fat diet-induced obesity and enriches fucoidan-degrading gut bacteria. *Carbohydr. Polym.* **2022**, *290*, 119411. [CrossRef]
60. Zhang, X.; You, Y.; Wang, L.; Ai, C.; Huang, L.; Wang, S.; Wang, Z.; Song, S.; Zhu, B. Anti-obesity effects of Laminaria japonica fucoidan in high-fat diet-fed mice vary with the gut microbiota structure. *Food Funct.* **2022**, *13*, 6259–6270. [CrossRef]
61. Phatak, M.; Nair, B.; Soni, U.; Pujari, R. Exploring the gut-brain axis: Microbiome contributions to pathophysiology of attention deficit hyperactivity disorder and potential therapeutic strategies. *Curr. Drug Metab.* **2025**, *26*, 1–11. [CrossRef]
62. Maghzi, A.-H.; Weiner, H.L. A One-Two Punch in the Gut May Trigger Multiple Sclerosis. *Immunity* **2020**, *53*, 707–709. [CrossRef] [PubMed]
63. Kong, Q.; Wang, B.; Tian, P.; Li, X.; Zhao, J.; Zhang, H.; Chen, W.; Wang, G. Daily intake of *Lactobacillus* alleviates autistic-like behaviors by ameliorating the 5-hydroxytryptamine metabolic disorder in VPA-treated rats during weaning and sexual maturation. *Food Funct.* **2021**, *12*, 2591–2604. [CrossRef]
64. Gandhi, D.N.; Pande, D.N.; Harikrishna, A.; Advilkar, A.; Basavan, I.; Ansari, R. Beyond the Brain: Attention Deficit/Hyperactivity Disorder and the Gut-Brain Axis. *Cureus* **2024**, *16*, e76291. [CrossRef]
65. MacDonald, H.J.; Kleppe, R.; Szigetvari, P.D.; Haavik, J. The dopamine hypothesis for ADHD: An evaluation of evidence accumulated from human studies and animal models. *Front. Psychiatry* **2024**, *15*, 1492126. [CrossRef]
66. Fu, J.; Li, J.; Sun, Y.; Liu, S.; Song, F.; Liu, Z. An integrated study on the comprehensive mechanism of *Schisandra chinensis* polysaccharides mitigating Alzheimer's disease in rats using a UPLC-Q-TOF-MS based serum and urine metabolomics strategy. *Food Funct.* **2023**, *14*, 734–745. [CrossRef]

67. Zhao, H.; Liu, J.; Wang, Y.; Shao, M.; Wang, L.; Tang, W.; Wang, Y.; Li, X. Polysaccharides from sea buckthorn (*Hippophae rhamnoides* L.) berries ameliorate cognitive dysfunction in AD mice induced by a combination of d-gal and AlCl3 by suppressing oxidative stress and inflammation reaction. *J. Sci. Food Agric.* **2023**, *103*, 6005–6016. [CrossRef] [PubMed]
68. Sun, Y.; Zeng, X.; Liu, Y.; Zhan, S.; Wu, Z.; Zheng, X.; Zhang, X. *Dendrobium officinale* polysaccharide attenuates cognitive impairment in circadian rhythm disruption mice model by modulating gut microbiota. *Int. J. Biol. Macromol.* **2022**, *217*, 677–688. [CrossRef] [PubMed]